



Technoeconomic analysis of biogas production using simple and effective mechanistic model calibrated with biomethanation potential experiments of water lettuce (*pistia stratiotes*) inoculated by buffalo dung



Gaurav Nahar ^a, Shailendrasingh Rajput ^b, Oliver Grasham ^c, Vishwanath Haily Dalvi ^{b,*}, Valerie Dupont ^c, Andrew B. Ross ^c, Aniruddha B. Pandit ^b

^a Defiant Renewables Pvt. Ltd., India

^b Department of Chemical Engineering, Institute of Chemical Technology, Mumbai, India

^c School of Chemical and Process Engineering, University of Leeds, Leeds, LS2 9JT, UK

ARTICLE INFO

Article history:

Received 15 August 2020

Received in revised form

23 November 2021

Accepted 11 December 2021

Available online 15 December 2021

Keywords:

Biomethanation

Pistia stratiotes

Buffalo dung

Biogas

Mechanistic model

Technoeconomic analysis

ABSTRACT

While many papers report biomethanation potential of various substrates subjected to various treatments, very few report the economic implications of their work. Here, we report a simple but effective mechanistic model, using Contois and Monod kinetics, considering only two classes of micro-organisms (a) acidogens and (b) acetomethanogens. We fitted our model to CH₄ and CO₂ evolution data from biomethanation studies of water lettuce (*pistia stratiotes*) inoculated with buffalo dung at five different ratios of substrate to inoculum. The data was obtained by gas chromatography. The model has been used to simulate three types of biodigestors: (a) 1-stage continuous digester, (b) 2-stage continuous digester and (c) semi-batch digester with intermittent draining of digestate. The 2-stage digester exhibited no major improvement over the 1-stage digester presenting only a 4% increase in methane production rate with 25% longer response times. The best performance was shown by the semi-batch operation due to tolerance of high microbial loads. Biogas generated from water lettuce grown on a farm pond and using the semi-batch approach can be monetized by offsetting use of market bought LPG. The return on investment is 24.7% and 25 kg of CO₂ emissions are abated per ton of water lettuce utilized.

© 2022 The Authors. Published by Elsevier Ltd. This is an open access article under the CC BY license (<http://creativecommons.org/licenses/by/4.0/>).

1. Introduction

There are many papers in the open literature that report on the biomethanation potential of various substrates subjected to various treatments. Very few papers, however, report on the economic implications of their work. However, technoeconomic analysis is critical for a cost-sensitive product like energy. A good economic analysis requires a reliable mechanistic model of biogas production: one that can relate gas generation to the composition of the liquid phase so that various bioreactors may be reliably sized/simulated and costed. While it is a daunting challenge to prepare a detailed mathematical model of a biodigester, here we report a simple but effective mechanistic model of biogas production from

Pistia Stratiotes (water lettuce) inoculated by buffalo dung.

Pistia Stratiotes or water lettuce is a pantropical invasive aquatic macrophyte. It is also called water cabbage, Nile cabbage, and shellflower. It is a known mosquito breeding habitat, causing serious clogging of waterways resulting from dense mats [1]. Water lettuce reduces water loss to evaporation by 20% and produces 2.4 tons of dry biomass per hectare per year [2]. Taking the average daily solar insolation to be 5 kWh/m² for tropical latitudes [3] and assuming a lower calorific value of biomass [4] of 15 MJ/kg, the solar-to-biomass efficiency of water lettuce is about 0.05% which is of the order of C3 plants [5]. However, if it is deliberately cultivated, it can yield a daily average of 5.8 g/m² of dry biomass [6] (i.e. efficiency of 0.48%). Terrestrial C4 grasses yield as much as 12 tons of dry biomass/hectare per year [7] (efficiency of 0.3%). Other aquatic macrophytes like water hyacinth (*Eichhornia crassipes*) yield 60–100 tons of dry biomass/hectare/year (efficiency of 1.4–2.5%).

* Corresponding author.

E-mail address: vh.dalvi@ictmumbai.edu.in (V.H. Dalvi).

Nomenclature		Yield Coefficients	
V_{hs}	m^3 Vapour headspace volume of the batch biomethanation reactors	Y_{acid}	unit-acidogen per kg substrate Units of acidogens produced upon consumption of 1 kg of substrate
V_{react}	m^3 Volume of liquid in a continuous biodigester	Y_{VFA}	unit-acetomethanogen per unit VFA Units of acetomethanogens produced upon consumption of 1 unit of VFA
P	Pa Pressure gauge reading	$Y_{CO_2}^{acid}$	kmolCO ₂ per kg substrate kmols of CO ₂ produced per kg of substrate metabolized by acidogens
T	K Temperature	$Y_{CO_2}^{meth}$	kmolCO ₂ per unit VFA Units of CO ₂ produced per unit of VFA metabolized by acetomethanogens
x	Mol Fraction in Vapour Phase	Y_{VFA}^{acid}	unit-VFA per kg substrate Units of VFA produced per unit of substrate metabolized by acidogens
n	kmols Number of kmols of a species	$Y_{CH_4}^{meth}$	kmolCH ₄ per unit VFA kmols of CH ₄ produced per unit of VFA metabolized by acetomethanogens
R	$J\ kmol^{-1}K^{-1}$ Universal gas constant (Value = 8314 $J\ kmol^{-1}K^{-1}$)	Initial Conditions	
N	kmols Number of kmols of a species generated	m_{BD}^0	kg of degradable substrate per kg of water lettuce
t	days Time elapsed since start of a run	m_{pistia}^0	kg of degradable substrate per kg of buffalo dung
Q	units Total units of microbes of a given species in a reactor at a given point of time.	m_{VFA}^0	kg of volatile fatty acids per kg of buffalo dung
r	Units per m^3 per second Volumetric rate of growth of microorganisms	q_{acid}^0	Units per kg Units of acidogens per kg of buffalo dung
F	kmols per day Gas production rate from a continuous biodigester	q_{meth}^0	Units per kg Units of acetomethanogens per kg of buffalo dung
A	m^2 Area	Rates of Addition to Continuous Biodigester	
p_r	$kg\ m^{-2}\ day^{-1}$ Production rate of fresh water lettuce	R_{pistia}	$kg\ day^{-1}$ Rate of addition of fresh water lettuce to a continuous biodigester
h_{rat}	Height to Diameter ratio of continuous biodigester	R_{dung}	$kg\ day^{-1}$ Rate of addition of fresh buffalo dung to a continuous biodigester
m	Thickness	$R_{inoculum}$	$kg\ day^{-1}$ Rate of addition of recycled effluent of continuous biodigester
c	$\$ kg^{-1}$ Purchase cost	R_{dil}	$kg\ day^{-1}$ Rate of addition of dilution water
d	m Diameter of a vessel	Subscript	
C	$\$$ Cost	CH ₄	Pertaining to Methane
Y	days Number of days in a year when a continuous biodigester is operational	CO ₂	Pertaining to Carbon Dioxide
Rol	Return on investment	VFA	Pertaining to VFA (volatile fatty acids)
Greek		0	Pertaining to the ambient
δ	When prefixed to a variable, it indicates the uncertainty associated with that variable e.g. δV is the uncertainty associated with the variable V	acid	Pertaining to acidogenesis
ρ	$kg\ m^{-3}$ Liquid Density	meth	Pertaining to acetomethanogenesis
τ	day^{-1} Dynamic Response time of a biodigester	react	Pertaining to a continuous bioreactor
η	Equivalency between calorific values of Methane and LPG	ss	Pertaining to Steady State
Kinetic Parameters		pond	Pertaining to a farm pond
μ_m^{acid}	$days^{-1}$ Maximum rate parameter for Contois Kinetics of acidogenesis	vessel	Pertaining to the continuous biodigester
K_s^{acid}	$kg\ units^{-1}$ Parameter of Contois Kinetics for acidogenesis	steel	Pertaining to the material of construction of the biodigester
μ_m^{meth}	$days^{-1}$ Maximum rate parameter for Monod Kinetics of acetomethanogenesis	fluid	Pertaining to the liquid phase
K_s^{meth}	$units\ m^{-3}$ Parameter of Monod Kinetics for acetomethanogenesis	LPG	Pertaining to Liquefied Petroleum Gas
Concentrations		Superscript	
X_{acid}	$units\ m^{-3}$ Volumetric Concentration of Acidogens in Liquid Phase	(n)	Pertaining to the n^{th} reading for a given run
X_{meth}	$units\ m^{-3}$ Volumetric Concentration of Acetomethanogens in Liquid Phase	i	Dummy Index
S	$kg\ m^{-3}$ Volumetric Concentration of Degradable Substrate in the Liquid Phase	cum	Pertaining to cumulative values since the start of a run or a simulation
S_{VFA}	$units\ m^{-3}$ Volumetric Concentration of Volatile Fatty Acid in arbitrary units	fluid	Pertaining to the fluid phase
		max	Pertaining to the maximum value of a variable
		min	Pertaining to the minimum value of a variable

Nevertheless, given the productivity on water bodies and the widespread availability of water-lettuce in energy-deprived regions of the world, it has been investigated for biogas production [8] and

also for phytoremediation of aqueous effluents [9]. The methanogenic activity of the water lettuce was not affected by heavy metal contamination [10]. Phytoremediation using water lettuce was

shown to treat water very effectively in only 7 days with as much as 88% COD removal, 99% ammonium nitrogen removal and 93% phosphate removal [6].

The high biodegradability of water-lettuce makes it interesting for biogas production [11]. It was found that inoculum was necessary for biogas production from water lettuce [8] since only water lettuce without inoculum yielded only carbon dioxide. The average methane content from water lettuce digestion using digested cattle manure as a source of microorganisms was found to be between 58 and 68% with as much as 83–99% of the volatile solids being biodegraded [11]. To fully understand the potential of biogas production from water lettuce it is important to design a reactor or reactor configurations suitable for producing large quantities of biogas from water lettuce in a continuous manner. The design will help in sizing of the phytoremediation system and utilizing the biomass generated effectively: increasing the productivity and efficiency of the system.

Recent work involves kinetic studies of biogas production from water lettuce [12] which fitted the methane production to a Monod and a Haldane kinetic model. The gold standard for kinetic modelling of biogas production is the Anaerobic Digestion Model 1 (ADM1) of the International Water Association (IWA) [13]. A review of model selection is available [14] which lists models for fitting batch, continuous and initial rate experiments. Another review [15] describes the various approaches to modelling anaerobic digestion processes including mechanistic models, ADM1, data-driven models and black-box approaches. However, simple mechanistic models have shown great success in predicting biogas yields and bio kinetics [16].

For most substrates, however, a phenomenological model (like the Gompertz curve) is fitted to batch experiments conducted in the AMPTS-II apparatus (or similar [17]) to obtain a biochemical methanation potential (BMP) e.g. see the work by Seswoya et al. [18]. Such experiments are excellent for rapidly screening substrates and inocula. However, they do not yield data necessary to carry out biomethanation equipment sizing. For this, we need a mechanistic model which relates biogas formation rate to the contents of the liquid media. A large number of BMP tests are available in the literature as reported in the review by Jingura et al. [19].

This work examines the biomethanation potential using pressure build-up in hermetically sealed bottles with gas composition measured offline using gas-chromatography. This is described in detail in the experimental methodology section. The great advantage of this method is that it yields quantitative numbers for carbon dioxide as well as methane evolution. It also allows assessing the dynamics of the system and monitoring the physico-chemical changes that are occurring in the process. This has allowed us to fit a mechanistic model assuming two populations of microorganisms: (a) acidogens that convert the substrate to carbon dioxide and volatile fatty acids and (b) acetomethanogens that convert the volatile fatty acids to carbon dioxide and methane. The model assumptions and governing equations are presented in the Mechanistic Model section. The goodness of the fit and the suitability of water lettuce as a feedstock for biomethane production from a technoeconomic perspective are covered in Results and Discussion.

2. Experimental methodology

Biochemical methanation potential of fresh water-lettuce with buffalo dung as inoculum was obtained using batch tests. The schematic of the experimental setup is shown in Fig. 1. Each experiment was performed in a 1100 ml reagent glass reactor (see Fig. 2) with a hermetically sealable specially machined Dearlin lid. The lid was fitted with a pressure gauge and a valved release tube. Every experiment was performed using fresh buffalo dung and chopped water lettuce plants added to a 400 ml of media containing nitrogen source of 5 g/l, 4.5 g/l of sodium chloride, 2 g/l of calcium carbonate and 2.5 g/l of yeast extract. The nitrogen source of the media was provided by supplying 2.5 g of tryptone and 2.5 g of urea per litre of digestion mixture. Based on the feed to inoculum ratio the amount of dung was varied keeping the biomass quantity constant at 10 g. A control bottle was used containing just 20 gm of buffalo dung. The other bottles held 10 gm of fresh water lettuce along with 20 gm, 15 gm, 10 gm and 7 gm of buffalo dung. The various batch runs, called A-E, are listed in Table 1.

The buffalo dung, water lettuce and medium were added to each bottle and diluted to 400 ml (see the schematics in Fig. 3). Near Neutral pH of the reactors was maintained. The bottles (5 in all) were then hermetically sealed with the Teflon lids. Each bottle was

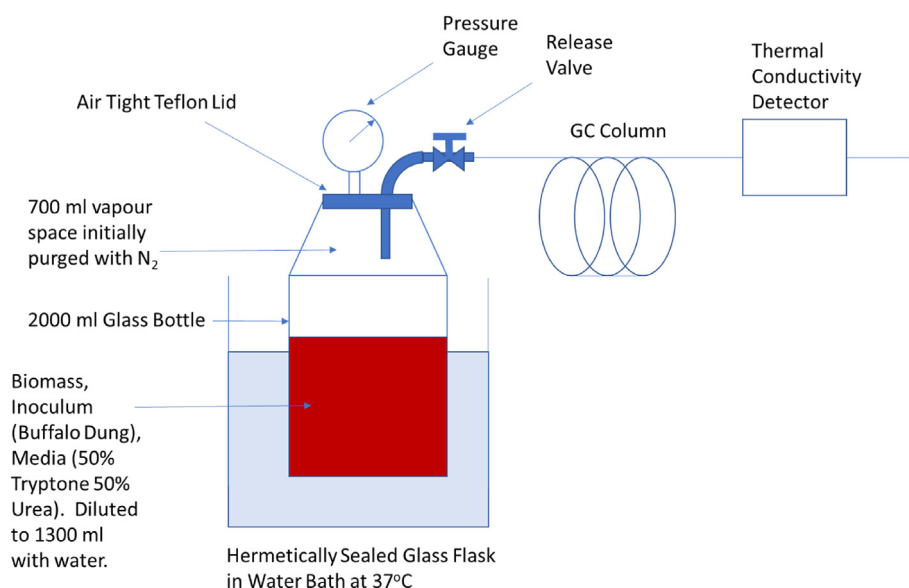


Fig. 1. Schematic of the experimental setup used in Biomethane potential analysis.



Fig. 2. Biomethanation Potential apparatus reactor with hermetically sealed Teflon lid fitted with a pressure gauge and release tube.

Table 1

The various batch runs carried out in this work.

Run	Quantity of Fresh Buffalo Dung (g)	Quantity of Fresh Water Lettuce (g)
A	20	0
B	20	10
C	15	10
D	10	10
E	7	10

leak tested by pressurizing with nitrogen and monitoring any overnight drop in pressure. The nitrogen gas was vented after a successful leak test. Leak tested reactors were placed in a water bath maintained at 37 °C and stirred twice a day. Upon evolution of gases (carbon dioxide and methane), the pressure in the bottles rises as noted from the pressure gauge. When the pressure in the 700 ml vapour phase reaches about 1.5 bar absolute (or 0.5 bar above ambient), the bottles are taken to a gas-chromatograph (GC, Agilent 7890 B Ga Chromatograph and the pressure in the reactors was released into the chromatography column through the release valve. Argon was used as a carrier gas for the GC and detection was performed by means of a thermal conductivity detector though a flame ionization detector was also available if needed. The monitoring of methane, oxygen and nitrogen was performed using molecular sieve 1/8" diameter with 9' length packed column. Carbon dioxide was measured using a 1/8" diameter packed HaySep Q with 16' length. The GC was equipped with gas sampling and

isolation valves which prevent the entry of carbon dioxide in the molecular sieve column preventing fouling and damage of molecular sieve column. The GC was quite sensitive and even small amount gas was enough for analysis. Methane and carbon dioxide mol fractions in the vapour space were thus detected.

The cumulative methane and carbon dioxide production from a batch was calculated from the results of the gas chromatography, using the ideal gas law. To explain the calculation procedure, certain terms must be defined. Let $V_{hs} = 0.0007 \text{ m}^3$ be the vapour head-space volume. Let $P^{(n)}$ be the pressure at the n^{th} reading. Note that this was not the n^{th} day's reading, but the n^{th} reading: the readings are not spaced evenly across time. Temperature $T = 37 + 273.16 = 310.16 \text{ K}$. Let $x_{\text{CH}_4}^{(n)}$ and $x_{\text{CO}_2}^{(n)}$ be the mol fractions of methane and carbon dioxide at the n^{th} reading. Let $P_0 = 1.013 \times 10^5 \text{ Pa}$ be the ambient pressure which the system relaxes to after each release. Hence, $P^{(0)} = P_0$.

Using these terms, the calculation procedure is illustrated using the example of methane noting that it applies exactly to carbon dioxide as well. At a particular n^{th} reading, the molar amount of methane present in the vapour phase was given by:

$$n_{\text{CH}_4}^{(n)} = x_{\text{CH}_4}^{(n)} \frac{P^{(n)} V_{hs}}{RT} \quad (1)$$

Here, $R = 8314 \text{ J kmol}^{-1} \text{ K}^{-1}$ is the universal gas constant. This was not, however, the methane released during that time interval between the n^{th} and the $(n-1)^{\text{th}}$ readings. There was already some methane present in the vapour head space. This was calculated as follows:

$$n_{\text{CH}_4}^{((n-1)0)} = x_{\text{CH}_4}^{(n-1)} \frac{P_0 V_{hs}}{RT} \quad (2)$$

The molar amount of methane newly produced in the time interval between the n^{th} and the $(n-1)^{\text{th}}$ readings was therefore:

$$N_{\text{CH}_4}^{(n)} = n_{\text{CH}_4}^{(n)} - n_{\text{CH}_4}^{((n-1)0)} = \frac{V_{hs}}{RT} \left(x_{\text{CH}_4}^{(n)} P^{(n)} - x_{\text{CH}_4}^{((n-1)0)} P_0 \right) \quad (3)$$

The cumulative production of methane until time $t^{(n)}$ was therefore simply an addition

$$N_{\text{CH}_4}^{\text{cum}(n)} = \sum_{i=0}^n N_{\text{CH}_4}^{(i)} \text{ with } N_{\text{CH}_4}^{(0)} = 0. \quad (4)$$

2.1. Uncertainty analysis

The uncertainties in V_{hs} , T and $P^{(n)}$ are denoted by δV_{hs} , δT and $\delta P^{(n)}$ respectively. Hence the uncertainty in $N_{\text{CH}_4}^{(n)}$ was given by:

$$\delta N_{\text{CH}_4}^{(n)} = \sqrt{\left(\frac{\partial N_{\text{CH}_4}^{(n)}}{\partial V_{hs}} \delta V_{hs} \right)^2 + \left(\frac{\partial N_{\text{CH}_4}^{(n)}}{\partial T} \delta T \right)^2 + \left(\frac{\partial N_{\text{CH}_4}^{(n)}}{\partial P^{(n)}} \delta P^{(n)} \right)^2} \quad (5)$$

This simplifies, with some algebra, to:

$$\delta N_{\text{CH}_4}^{(n)} = N_{\text{CH}_4}^{(n)} \sqrt{\left(\frac{\delta V_{hs}}{V_{hs}} \right)^2 + \left(\frac{\delta T}{T} \right)^2 + \left(\frac{\delta P^{(n)}}{P^{(n)}} \right)^2} \quad (6)$$

The uncertainties are reported in Table 2.

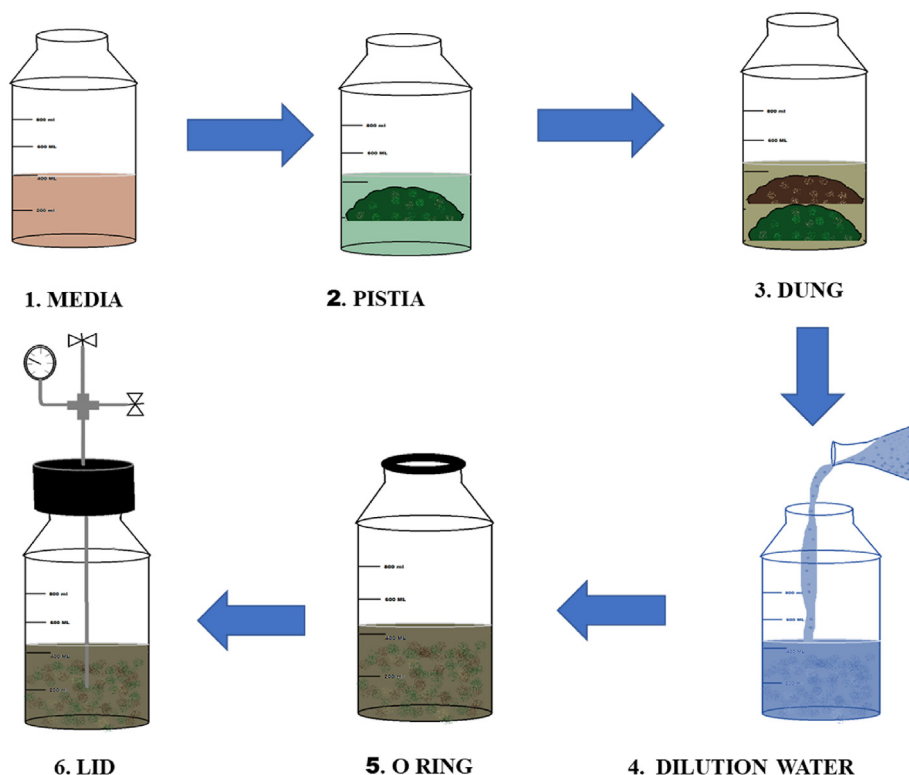


Fig. 3. Schematic of the preparation for a biomethane potential run.

Table 2
Uncertainties of various pertinent quantities.

Quantity	Symbol	Uncertainty
Vapour Head Space	V_{hs}	1 ml
Temperature	T	2 K
Pressure	$p^{(n)}$	0.1 bar

$$\delta N_{CH4}^{cum(n)} = N_{CH4}^{cum(n)} \sqrt{\sum_{i=0}^n \left(\frac{\delta N_{CH4}^{(i)}}{N_{CH4}^{(i)}} \right)^2} \quad (7)$$

An exactly analogous expression holds for carbon dioxide.

2.2. Mechanistic model

Lauwers et al. present an excellent review of mechanistic models for anaerobic digestion [15]. The actual process of biomethanation is extremely complex. However, it can be roughly divided into four parts, namely.

- (a) Hydrolysis where the substrate is degraded into simple sugars.
- (b) Acidogenesis where the sugars are converted to volatile fatty acids (VFAs) with the concomitant release of carbon dioxide
- (c) Acetogenesis where the VFAs are converted to acetates with the release of hydrogen and carbon dioxide. Hydrogen is inhibitory to acetogenesis but is constantly consumed in the subsequent methanogenesis step.
- (d) Methanogenesis where the acetates are converted to methane, and hydrogen and carbon dioxide are combined to form methane.

The various mechanistic models that are available in literature yield, as they should, a sigmoidal curve in the cumulative methane and carbon dioxide time plots. In this work, we were only measuring carbon dioxide and methane evolution. Hence, an extremely detailed model e.g. as suggested by ADM1 [13] is not tenable for the quality of data at hand.

Therefore, we propose a model with only two microbial consortia: (a) acidogens which hydrolyse the substrate and convert sugars to VFAs with the release of carbon dioxide and (b) acetomethanogens which convert the VFAs to methane and carbon dioxide. This type of categorization was reasonable to assume since the first two are driven by extracellular enzymes whereas the latter two are driven by intracellular enzymes. Thus the physico-chemical constraints to the molecular or species transport are expected to be similar for these two genres of microbes. The hydrogenotropic mechanism cannot be treated separately, but has to be bundled up with the overall methanogenesis, because hydrogen was not detected in the gas chromatography experiments. Hence, rather than introduce another hidden variable, it was decided to club both of the methane producing parts into one.

2.3. Differential equations

We assume the batch liquid to be well mixed: a reasonable assumption with, as we shall see later, much smaller time intervals between shaking than process time constants. Let X_{acid} (units/m³) be the concentration of acidogens at any point in time in the batch liquid. Let S (kg/m³) be the concentration of the substrate in the batch liquid. Since the substrate was solid, it was first engulfed by the acidogenic microorganisms that secrete degrading enzymes onto it. The particles of solid then degrade from the outside in. The process by which microbes grow is well described by Contois kinetics [20] i.e.

$$\frac{dX_{acid}}{dt} = \frac{\mu_m^{acid} S}{K_s^{acid} X_{acid} + S} X_{acid} \quad (8)$$

where μ_m^{acid} and K_s^{acid} are constants of the Contois Kinetics.

The acidogenesis generates VFAs and releases carbon dioxide. The VFAs are soluble in water and hence are accessible to microorganisms suspended in the solution. Consequently, the growth of microbes for acetomethanogenesis can be well represented by standard Monod kinetics. Hence, if X_{meth} (units/m³) is the concentration of acetomethanogens in the batch liquid, then, Monod kinetics predicts:

$$\frac{dX_{meth}}{dt} = \frac{\mu_m^{meth} S_{VFA}}{K_s^{meth} + S_{VFA}} X_{meth} \quad (9)$$

where S_{VFA} (units/m³) is the concentration of VFAs in the batch liquid and μ_m^{meth} and K_s^{meth} are constants of the Monod kinetics. Here it must be noted that the concentration of VFA is simply stated as units per cubic meter. This is because we have not measured VFA concentration in our experiment. Hence S_{VFA} is essentially a hidden variable in our analysis whose units are arbitrary.

As microbes grow, they consume the substrate and generate products of metabolism. The rate of consumption of the substrate is proportional to the microbial rate of growth. Hence,

$$\frac{dS}{dt} = -\frac{dX_{acid}}{dt} \frac{1}{Y_{acid}} \quad (10)$$

where Y_{acid} is the yield coefficient. It must be noted that, for matching dimensions, the yield coefficient is not a dimensionless number, but carries dimensions of its own.

Similarly, the rate of VFA production/consumption was given by:

$$\frac{dS_{VFA}}{dt} = \frac{dX_{acid}}{dt} \frac{Y_{VFA}^{acid}}{Y_{acid}} - \frac{dX_{meth}}{dt} \frac{1}{Y_{VFA}} \quad (11)$$

Here, the corresponding yield coefficients are Y_{VFA}^{acid} and Y_{VFA} .

The rate of production of carbon dioxide was given by:

$$\frac{dN_{CO_2}^{cum}}{dt} = V \frac{dX_{acid}}{dt} \frac{Y_{CO_2}^{acid}}{Y_{acid}} + V \frac{dX_{meth}}{dt} \frac{Y_{CO_2}^{meth}}{Y_{VFA}} \quad (12)$$

where $Y_{CO_2}^{acid}$ is the yield coefficient for carbon dioxide during acidogenesis and $Y_{CO_2}^{meth}$ is the corresponding yield coefficient during acetomethanogenesis. V is the volume of the liquid phase.

Finally, the rate of production of methane was given by:

$$\frac{dN_{CH_4}^{cum}}{dt} = V \frac{dX_{meth}}{dt} \frac{Y_{CH_4}^{meth}}{Y_{VFA}} \quad (13)$$

where $Y_{CH_4}^{meth}$ was the corresponding yield coefficient of methane during acetomethanogenesis.

Consequently, there 10 parameters in all determined by regression:

- 4 kinetic parameters: μ_m^{acid} , K_s^{acid} , μ_m^{meth} , K_s^{meth}
- 3 yield coefficients of acidogenesis: Y_{acid} , $Y_{CO_2}^{acid}$, Y_{VFA}^{acid}
- 3 yield coefficients of acetomethanogenesis: Y_{VFA} , $Y_{CO_2}^{meth}$, $Y_{CH_4}^{meth}$

2.4. Initial conditions

The only experimental measurements utilized are the quantities of methane and carbon dioxide produced in the biomethanation bottle, the volumes of gas and liquid phase and the quantities of fresh dung and water lettuce added to the bottle. These figures do not include important quantities like the number of units of the microorganisms or the quantities of substrate and VFAs that might be initially present in the dung. These are difficult to determine. Although volatile solids may be considered a proxy for digestible substrate, there is no simple method of determining microbial amount other than CFM tests: and even these cannot distinguish between the microbial consortia.

Consequently, it was decided to determine the initial quantities of the substrate as well as units of the acidogens and acetomethanogens initially present in the dung by regression.

The initial values to be determined are as follows:

m_{BD}^0 = kg of substrate per kg of buffalo dung.

m_{pistia}^0 = kg of substrate per kg of water lettuce.

m_{VFA}^0 = kg of VFA per kg of buffalo dung.

q_{acid}^0 = units of acidogens per kg of buffalo dung.

q_{meth}^0 = units of acetomethanogens per kg of buffalo dung.

2.5. Regression

For regression, the 10 model parameters are kept constant across runs while the 5 initial conditions are specific to each run. Since there are 5 runs, we are regressing for 35 parameters in all. Ideally, the 5 initial parameters should themselves be constant across runs. However, since the study uses freshwater lettuce and fresh cow dung, batch to batch variation across runs exist and must be accounted for.

With initial guess estimates of the model parameters and initial values, the sets of simultaneous ordinary differential equations are solved using a marching method (using the SciPy([21]) package of the Python 3 programming environment) to retrieve estimates of $N_{CH_4}^{cum(n)}$ and $N_{CO_2}^{cum(n)}$ for a time $t^{(n)}$ at which these same values are measured.

The regressed values of the parameters are obtained using a "trust region reflective" algorithm([22]) also implemented in the SciPy package. This algorithm takes, as input, the list of the differences between $N_{CH_4}^{cum(n)}$ and $N_{CO_2}^{cum(n)}$ as measured experimentally and as evaluated from the model and returns a set of parameters that minimizes a cost function of these differences. The general philosophy of the regression was similar to that used in Ref. [23].

3. Results and Discussion

The experimental results and results of the model fit are illustrated in Fig. 4 (and Appendix A of the Supporting Information). The fits are very good indicating the strength of the mechanistic model. From Fig. 4, it is clear that there is a significant lag (of almost a month) in the production of methane i.e. acetomethanogenesis. However, once methane production starts, it saturates in only 20 days. This can be interpreted as the microorganisms becoming acclimatized to the environment of the batch runs. However, in the context of the mechanistic model, this was interpreted as a much lower initial population of acetomethanogens compared to acidogens (see Table 4) which over a period of a month were established enough to start producing methane in measurable quantities. It was of interest to see that the quantity of degradable substrate was estimated from the regression fit to be about 10% in the buffalo dung as well as in the water lettuce. This was very

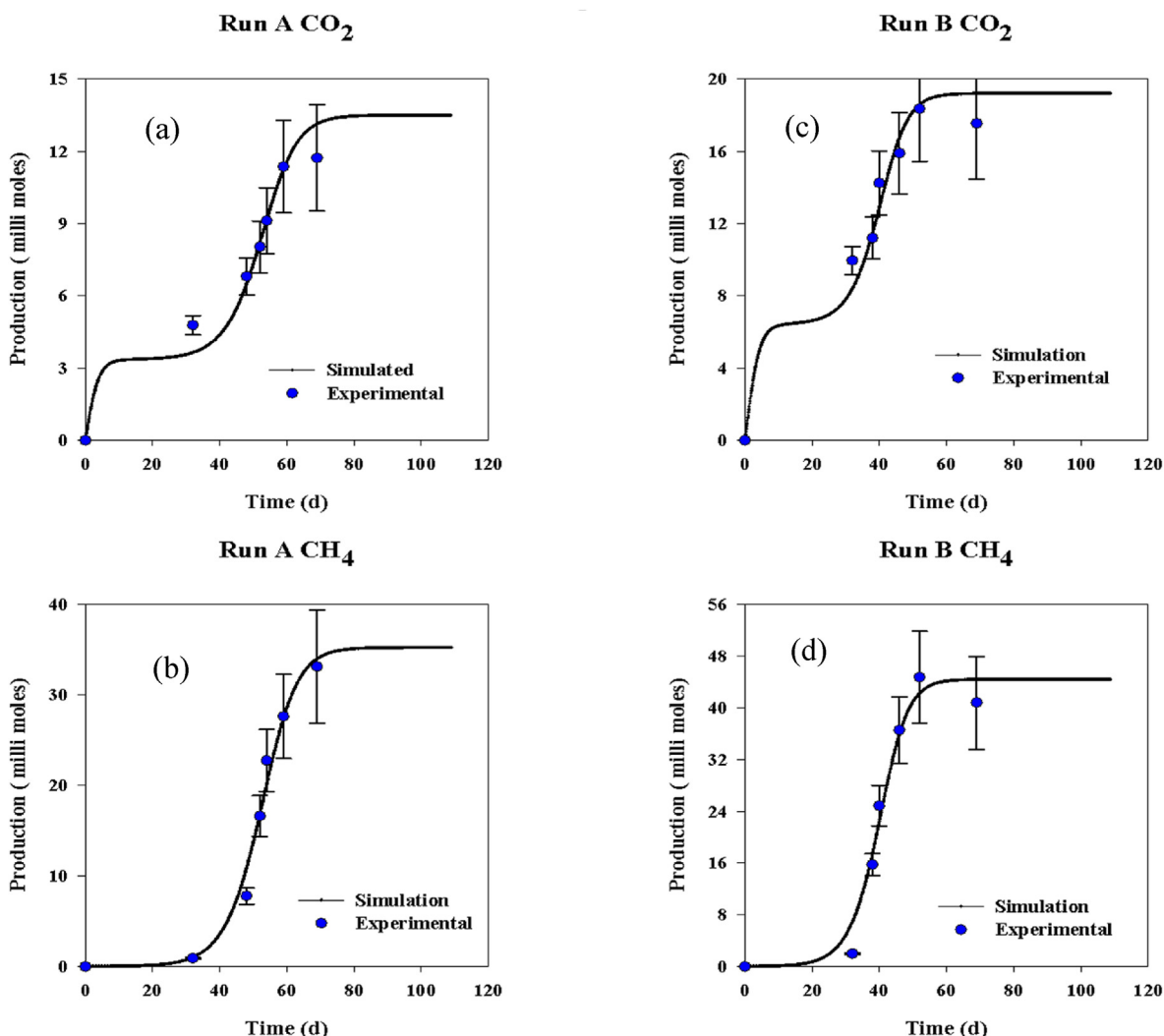


Fig. 4. Experimental results (dots with standard error bars) superimposed with results of the fitted model (solid lines). (a) CO₂ for Run A (see Table 1), (b) CH₄ for Run A, (c) CO₂ for Run B and (d) CH₄ for Run B. For Runs C-E, please refer to Appendix A of the Supporting Information.

Table 3

Fitted model parameters (see Section 3 for related equations).

Model Parameter	Value
μ_m^{acid}	0.603 d ⁻¹
μ_m^{meth}	0.766 d ⁻¹
K_s^{acid}	1.11 kg/unit-acidogens
K_s^{meth}	2.34 unit-VFA/m ³
Y_{acid}	1.11 unit-acidogen/kg-substrate
Y_{VFA}	1.029 unit-acetomethanogen/unit-VFA
$\gamma_{CO_2}^{acid}$	0.0015 kmolCO ₂ /kg-substrate
$\gamma_{CO_2}^{meth}$	0.0395 kmolCO ₂ /unit-VFA
γ_{VFA}^{acid}	0.0284 unit-VFA/kg-substrate
$\gamma_{CH_4}^{meth}$	0.137 kmolCH ₄ /unit-VFA

consistent with a water content of about 90% i.e. the bulk of the solids in the biomass are degradable. Part of the substrate was consumed by the microorganisms for their own growth while the remainder are used to produce carbon dioxide and methane. Since methane content in the final gas is an important parameter, the ratio of methane to carbon dioxides shown in Table 5. The water lettuce with cow dung inoculum produces a very high quality of

Table 4

Regressed initial values (see Section 3 for related equations).

Run	m_{BD}^0 kg/kg	m_{pistia}^0 kg/kg	m_{VFA}^0 kg/kg	a_{acid}^0 Units/kg	a_{meth}^0 Units/kg × 10 ⁶
A	0.1270	0.171	0.01010	0.1550	6.35
B	0.1110	0.163	0.00968	0.1060	2.16
C	0.1310	0.183	0.02180	0.0726	7.98
D	0.0469	0.120	0.01050	0.0581	143.00
E	0.1250	0.182	0.01830	0.1060	12.00
Average	0.1080	0.164	0.01410	0.0996	34.2

biogas with methane to carbon-dioxide ratio of about 2.4 i.e. a methane content of about 70% in the final biogas. This is relatable to methane contents of 58–68% which are already reported in literature(8).

Table 5 also shows the final microbial concentrations for the various runs. Unsurprisingly, once gas production has tapered off, the acidogens are an order of magnitude more numerous than the acetomethanogens. The maximum acidogen concentration was 19.6 units/m³ and the maximum acetomethanogen concentration

Table 5
CH₄/CO₂ ratios for the various runs and final microbial concentrations.

Run	CO ₂ produced Millimols	CH ₄ produced millimols	CH ₄ : CO ₂ ratio	Acidogen Concentration Units/m ³	Acetomethanogen Concentration Units/m ³
A	13.5	35.2	2.6	11.5	0.66
B	19.2	44.4	2.3	19.6	0.83
C	16.9	42.3	2.5	10.6	0.79
D	11.3	29.0	2.6	7.5	0.54
E	12.2	28.1	2.3	9.4	0.52

was 0.83 units/m³: both encountered in Run B: which has the highest biomass. At these concentrations, the liquid phase was free flowing slurry. The fitted model parameters are as shown in Table 3. The initial values are reported in Table 4. Table 5 shows the CH₄:CO₂ ratios and the microbial concentrations in the various runs.

From Table 3 the quantity of CH₄ generated per kg of substrate is given by $Y_{CH_4}^{meth} Y_{VFA}^{acid} = 0.00389 \frac{kmol}{kg \text{ substrate}}$. Hence the methane produced is 88 ml/gm-substrate.

3.1. Single stage continuous biodigester

The calibrated model can be used for reactor design. Continuous reactors come in two idealized categories ([24]) (a) the Continuous Stirred Tank Reactor (CSTR) and (b) the Plug Flow Reactor (PFR). The CSTR is a tank which is assumed ideally well mixed and is the idealized reactor for most reactors where the raw materials are input continuously and directly into a well stirred fluid mixture and an equivalent volume of the well stirred mixture is continuously withdrawn. The PFR can be visualized as a pipe where continuous “plugs” or packets of raw materials are inserted at one end and leave the opposite end after a set amount of time. The performance of a PFR is identical to the performance of a batch reactor with batch time equal to the residence time in the PFR.

Of the two types of reactors, the stirred tank is the easiest to deploy, which is why the bulk of anaerobic digesters are of this type [25]. The idealized stirred tank is the CSTR. The mechanistic model was therefore used to explore the behaviour of water lettuce inoculated with buffalo dung in a CSTR.

Fig. 5 shows a schematic of a continuous stirred biogas digester which was modelled as a stirred tank. Fresh water lettuce, dilution water and fresh buffalo dung are continuously added to the digester along with a portion of the effluent recycled as inoculum. The liquid level in the tank is maintained by constantly withdrawing digestate as effluent and the biogas produced is constantly withdrawn from the vapour head space.

To simulate the behaviour of a continuous biodigester, a set of differential equations must be written which are different enough from the equations set up and solved in the Experimental Methodology section. Since there are properly part of the discussion (rather than part of the experimental protocol), it is decided to present them in the Results and Discussion section.

Accordingly, let V_{react} be the volume of the liquid in the reactor. Let Q_{acid} be the quantity of acidogens (units) present in the CSTR at any point of time and let Q_{meth} be the quantity of the acidomethanogens (units). Let R_{pistia} , R_{dung} and $R_{inoculum}$ be the rates of addition of fresh water lettuce, fresh dung and recycled inoculum in kg/day. Let R_{dil} be the rate of addition of dilution water in kg/day. Let $\rho = 1000 \text{ kg/m}^3$ be the density of water as well as the water lettuce, dung and inoculum (all of which are mostly water).

Let $X_{acid} = Q_{acid}/V_{react}$ be the concentration of the acidogens in the reactor and let $X_{meth} = Q_{meth}/V_{react}$ be the concentration of the acetomethanogens in the reactor. Hence, the volumetric rate of

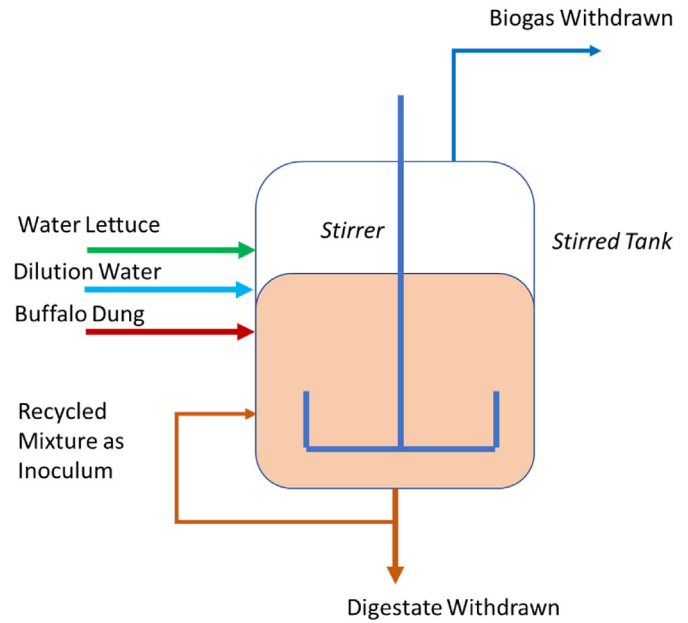


Fig. 5. Schematic of a single stage biogas digester modelled as a CSTR.

growth of the acidogens is (analogous to equation [8]):

$$r_{acid} = \frac{\mu_m^{acid} S}{K_s^{acid} X_{acid} + S} X_{acid} \quad (14)$$

where S is the concentration of the substrate given by $S = N_s/V_{react}$ where N_s is the total molar volume of substrate in the reactor at any point of time. μ_m^{acid} and K_s^{acid} have the same meaning as they do in equation [8] and their values are in Table 3.

Hence,

$$\frac{dQ_{acid}}{dt} = R_{dung} Q_{acid}^0 - \frac{R_{pistia} + R_{dung} + R_{dilution}}{\rho} X_{acid} + r_{acid} V_{react} \quad (15)$$

Similarly, the volumetric rate of growth of the methanogens was (analogous to equation [9]):

$$r_{meth} = \frac{\mu_m^{meth} S_{VFA}}{K_s^{meth} + S_{VFA}} X_{meth} \quad (16)$$

where S_{VFA} was the concentration of the volatile fatty acids given by $S_{VFA} = N_{VFA}/V_{react}$ and N_{VFA} is the total quantum of volatile fatty acids in the reactor at any point of time. μ_m^{meth} and K_s^{meth} have the same meaning as they do in equation [9] and their values are represented in Table 3.

Hence,

$$\frac{dQ_{meth}}{dt} = R_{dung}q_{meth}^0 - \frac{R_{pistia} + R_{dung} + R_{dilution}}{\rho} X_{meth} + r_{meth}V_{react} \quad (17)$$

where q_{meth}^0 is obtained from Table 4.

The substrate balance is as follows:

$$\frac{dN_S}{dt} = R_{dung}n_{BD}^0 + R_{pistia}n_{pistia}^0 - \frac{R_{pistia} + R_{dung} + R_{dilution}}{\rho} S - r_{acid}V_{react}\frac{1}{Y_{acid}} \quad (18)$$

Here n_{BD}^0 and n_{pistia}^0 are obtained from Table 4 and Y_{acid} from Table 3.

The VFA balance is as follows:

$$\frac{dN_{VFA}}{dt} = R_{dung}n_{VFA}^0 - \frac{R_{pistia} + R_{dung} + R_{dilution}}{\rho} S_{VFA} + r_{acid}V_{react}\frac{Y_{VFA}^{acid}}{Y_{acid}} - r_{meth}V_{react}\frac{1}{Y_{VFA}} \quad (19)$$

Here n_{VFA}^0 is obtained from Table 4 and Y_{VFA}^{acid} from Table 3.

The carbon dioxide balance is as follows:

$$\frac{dN_{CO2}}{dt} = r_{acid}V_{react}\frac{Y_{CO2}^{acid}}{Y_{acid}} + r_{meth}V_{react}\frac{Y_{CO2}^{meth}}{Y_{VFA}} \quad (20)$$

Here Y_{CO2}^{acid} and Y_{CO2}^{meth} are obtained from Table 3.

Finally, the CH₄ balance is as follows:

$$\frac{dN_{CH4}}{dt} = r_{meth}V_{react}\frac{Y_{CH4}^{meth}}{Y_{VFA}} \quad (21)$$

Here Y_{CH4}^{meth} was obtained from Table 3.

The reactor begins with a volume (V_{react}) of 1 m³ of liquid phase containing plain water and an added feed consisting of $R_{pistia} = 5$ kg/day, $R_{dung} = 0.5$ kg/day, $R_{inoculum} = 0.5$ kg/day and $R_{dilution} = 50$ kg/day. Fig. 6 shows how the two microbial consortia of acidogens

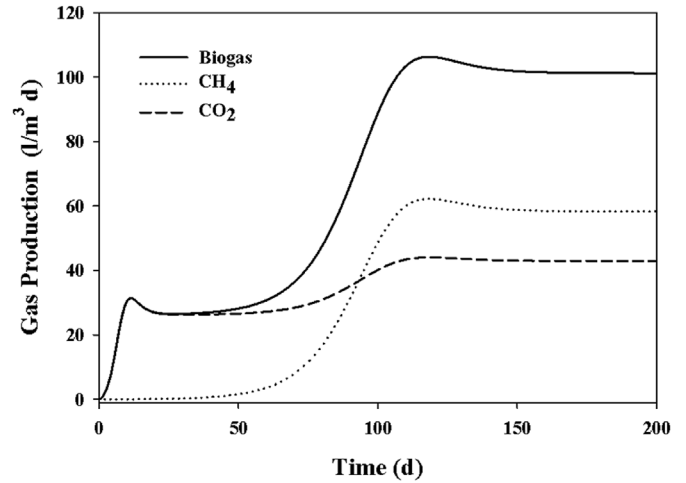


Fig. 7. Biogas, methane and carbon dioxide production rates as a function of time in the single stage digester.

and acetomethanogens establish themselves over time. Steady state was reached in about 150 days with acidogen concentration stabilizing at 16.4 Units/m³ and acetomethanogen concentration stabilizing at 0.35 Units/m³.

Fig. 7 shows the biogas production rates for this system. Upon stabilization, the steady state gas production rate was 101 l-biogas/m³-digester/day with a methane composition of 58%. It is very interesting to see a peak in the gas production at about 120 days: just before stabilization. The hydraulic retention time can be varied by changing the feed rate of water lettuce for a given rate of dilution water flow rate.

Fig. 8 shows the effect of the microbial concentration in the reactor at steady state for various hydraulic retention times as varied by changing the feed rate of fresh water lettuce. The rate of dilution waterways varied between 10, 20 and 50 kg/day as highlighted in the legend of Fig. 8. Fig. 9 shows the corresponding methane production. A strong correlation exists between microbial concentration and methane production. However, the microbial

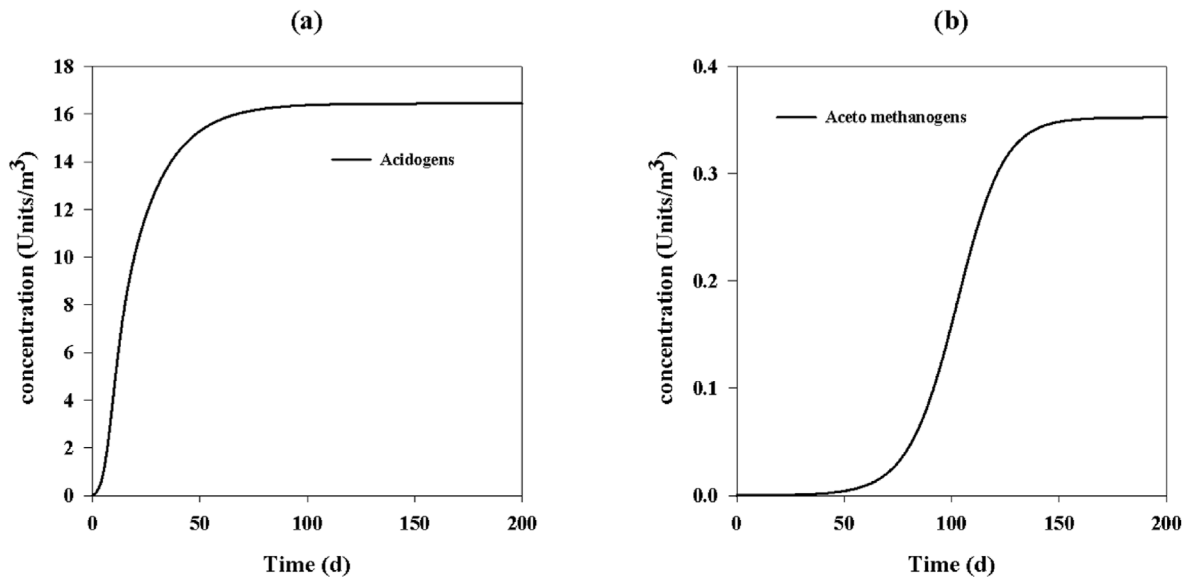


Fig. 6. Concentration of microbial consortia in units per m³ as a function of time in a single stage CSTR (a) Concentration of acidogens which stabilizes at 16 Units/m³ and (b) Concentration of acetomethanogens which stabilizes at 0.35 Units/m³.

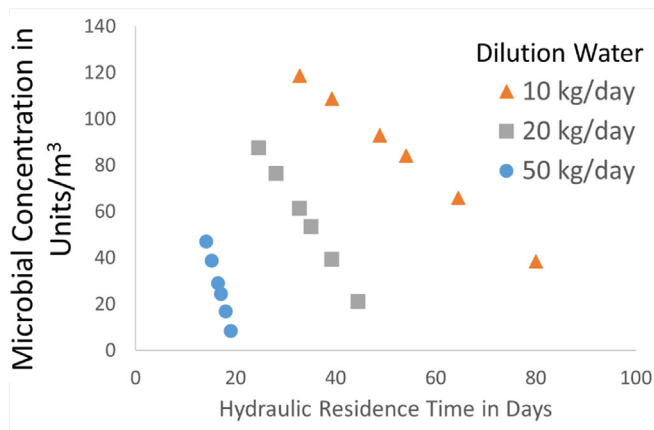


Fig. 8. Microbial Concentration as a function of hydraulic residence time as varied by water lettuce addition. The dilution water addition rate was the parameter.

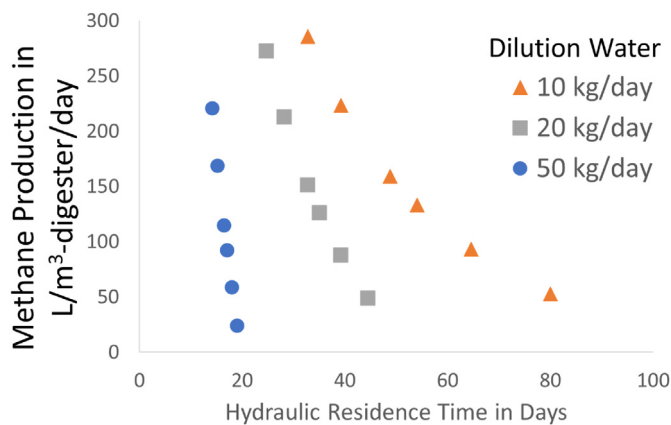


Fig. 9. Methane production as a function of hydraulic residence time is varied by water lettuce addition. The dilution water addition rate was the parameter.

concentration faces an upper limit due to the viscosity and flowability of the solution. If the microbial counts encountered in the laboratory experiments (about 20 Units/m³) were used, then the expected biogas production was between 100 and 150 L/m³-digester/day with a methane concentration of about 58% v/v. This was achieved with a dilution rate of 50 kg/day of dilution water and a water lettuce feed rate between 5 and 8 kg/m³-digester/day.

Buffalo dung is a better feed for methane productions compared to water lettuce, as can be seen from Fig. 10. For a dilution rate of 50 kg/day of dilution water, the rate of biogas production with buffalo dung was between 260 and 290 L/m³-digester/day with a methane component of 72% v/v while with a water lettuce to dung ratio of 10:1, it is only about 90–100 L/m³-digester/day with a methane component of 57% v/v. In all cases with 50 kg/day dilution rate, the microbial concentration remains below 20 units/m³.

3.2. Two stage continuous biodigester

Since the microbial count determined the upper limit to the productivity of a single stage biodigester fed primarily with water lettuce (and not buffalo dung), a two stage biodigester might be promising. It was modelled as two CSTRs in series as shown schematically in Fig. 11.

The volume was set of the first reactor $V_{react}^{(1)} = 0.5 \text{ m}^3$ and that of

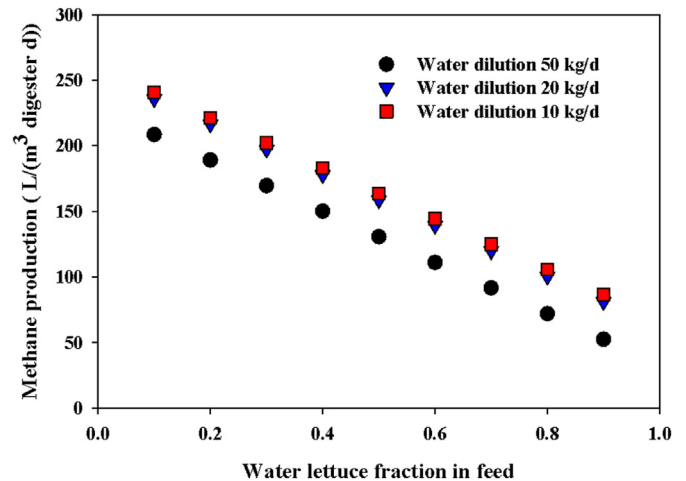


Fig. 10. Methane production when the fraction of water lettuce to buffalo dung is varied. The microbial concentration for each dilution rate is shown alongside the legend.

the second reactor $V_{react}^{(2)} = 0.5 \text{ m}^3$. The rate of water lettuce addition was $R_{pistia} = 5.0 \text{ kg/day}$, of dung was $R_{dung} = 0.5 \text{ kg/day}$, of inoculum $R_{inoculum} = 0.5 \text{ kg/day}$ (for both stages) and the rate of dilution water is $R_{dilution} = 50 \text{ kg/day}$. Upon running the dynamic model starting with a reactor filled with plain water, the microbial consortium is shown in Fig. 12 for acidogens and Fig. 13 for acetomethanogens. Although the acidogens establish themselves in less than 100 days, it takes more than 400 days for the acetomethanogens to reach steady state.

Fig. 14 shows gas production rates for the 2 stage digester with 0.5 m³ in the first stage and 0.5 m³ in the second stage. Contrary to expectation, the combined gas production rate is 91 l/m³-digester/day which is lower than that for the single stage digester (101 l/m³-digester/day) and the quality of methane is just 54 vol % against 58 vol % for the 1 stage digester.

Fig. 15 shows the effect of distributing volumes between the two stages. The abscissa shows the fraction of the total volume occupied by the first stage. If this number is 1 or 0, it implies a single stage digester. The behaviour is counterintuitive. It shows if the first stage occupies 80% of the total volume the methane production rate (at 57 vol % methane) was 60.6 l/m³-digester/day. This is a slight increase on 58.3 l/m³-digester/day for the single stage digester also at 57 vol % methane. Hence, for all the trouble with a 2 stage digester design, only a 4% improvement in methane production is obtained.

3.3. Response times

It is of interest to compare the response times of the two types of digesters. Starting with an operation at steady state with a feed of 5 kg/day water lettuce, 0.5 kg/day dung, 0.5 kg/day inoculum and 50 kg/day dilution water, a step change in water lettuce feed was executed at day 0–5.5 kg/day water lettuce. The response of the 1 m³ single stage CSTR and the 1 m³ two stage CSTRs in series (first stage occupying 80% of the volume) are compared. The dynamic responses of the two types of operation as they attain their new steady state are shown in Fig. 16. The responses are first order and given by:

$$F = F_{ss}^{(1)} + (F_{ss}^{(2)} - F_{ss}^{(1)}) (1 - e^{-t/\tau}) \quad (22)$$

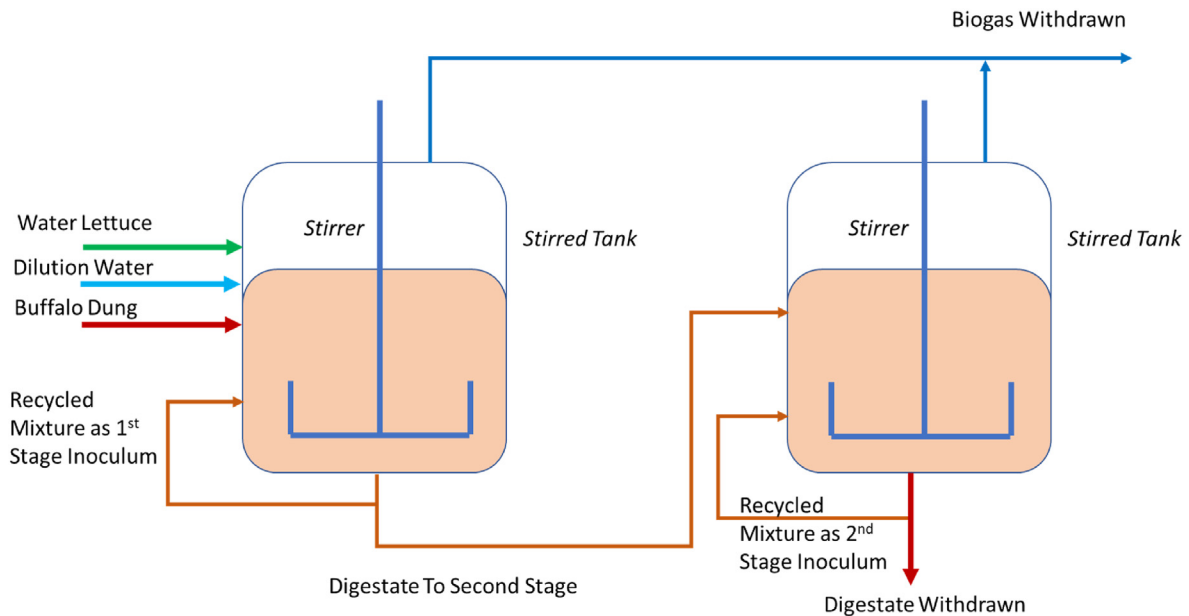


Fig. 11. Schematic of a two stage digester modelled as two CSTRs in series.

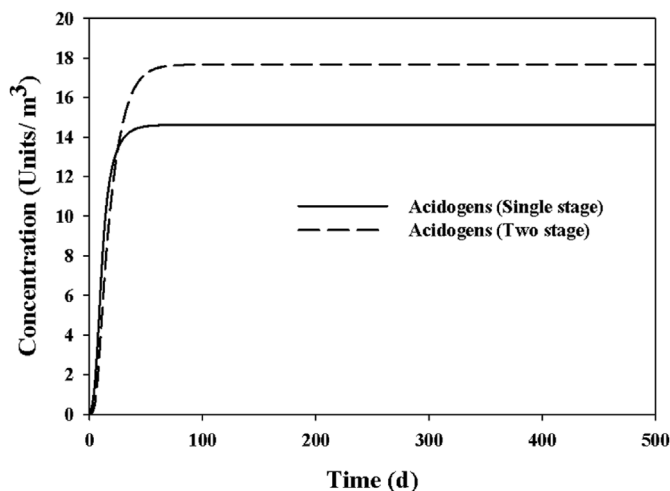


Fig. 12. Concentration of acidogens in stage 1 and stage 2 of the two stage reactor with each stage of 0.5 m³ volume.

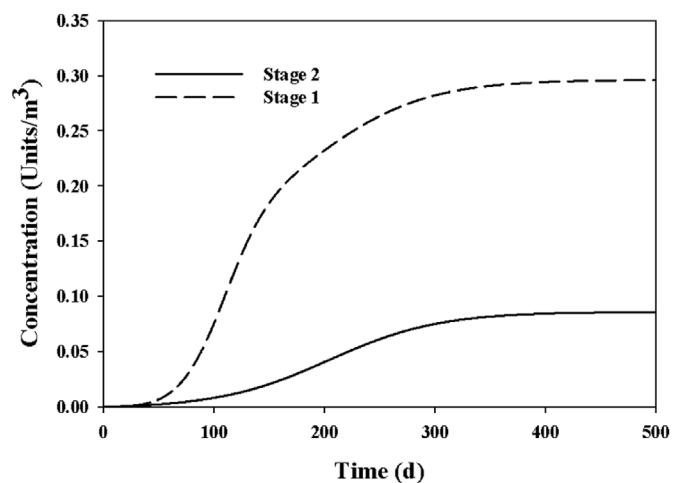


Fig. 13. Concentration of acetomethanogens in stage 1 and stage 2 of the two stage reactor with each stage of 0.5 m³.

where F is the gas production rate, $F_{ss}^{(1)}$ is the gas production rate at first steady state (i.e. at Day 0) and $F_{ss}^{(2)}$ is the gas production rate at the new steady state. t is the time in days and τ is the time constant in days. The single stage response time constant (τ) is 9.3 days while the two-stage response time is 11.6 days i.e. 25% longer.

3.4. Semi-batch digester

Continuous flow reactors present difficulties in operation and maintenance: they require sophisticated systems of control and actuation to run and the requirement of pumpability presents an upper limit to the microbial concentration in the reactors. On the other hand, batch reactors do not require pumping and hence can work with a much higher microbial concentration. Consequently,

the reactor can be operated in semi batch mode. Here, the reactor is fed continuously and biogas is withdrawn continuously, but the reactor fluid is withdrawn intermittently. Hence, upon starting the reactor, a feed of fresh water lettuce, dung, salt, limestone, nitrogen source etc is fed at a certain rate into a practically empty vessel. Whatever biogas is produced is withdrawn continuously. However, the contents of the reactor are not withdrawn until the reactor contents reach a maximum volume V_{max} . At this point the reactor contents are rapidly drawn down until the reactor volume reaches a set minimum value V_{min} after which withdrawal is stopped and the cycle repeats. Fig. 17 shows a schematic of the semi batch operation.

For an illustrative example of this process, consider a feed of fresh water lettuce of 5 kg/day mixed with buffalo dung at 0.5 kg/day added to a reactor with $V_{max} = 1 \text{ m}^3$ which is initially empty.

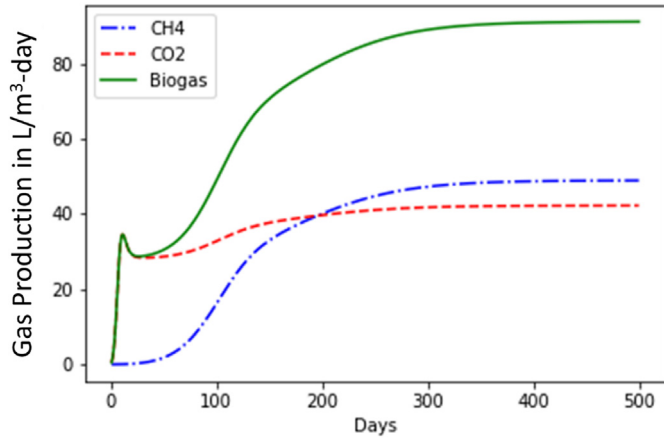


Fig. 14. Biogas, methane and carbon dioxide production rates as a function of time in the 1 m³ 2-stage digester. Each stage is 0.5 m³. The graph shows the combined gas production rate.

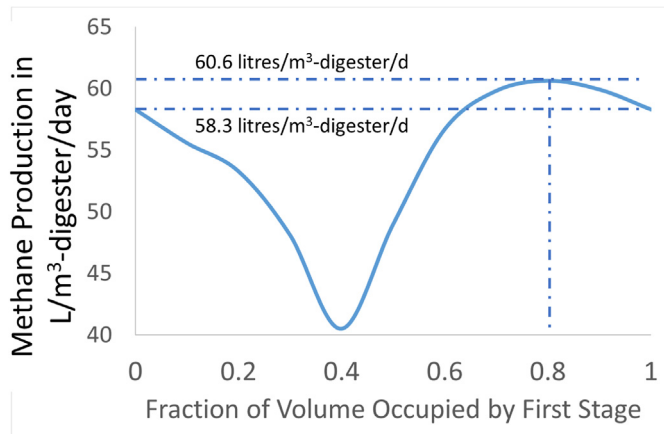


Fig. 15. Methane production rate as a function of the fraction of the total volume occupied by the first stage of the 2 stage digester. The total volume is 1 m³ of liquid. Volume fractions 0 or 1 imply single stage digester.

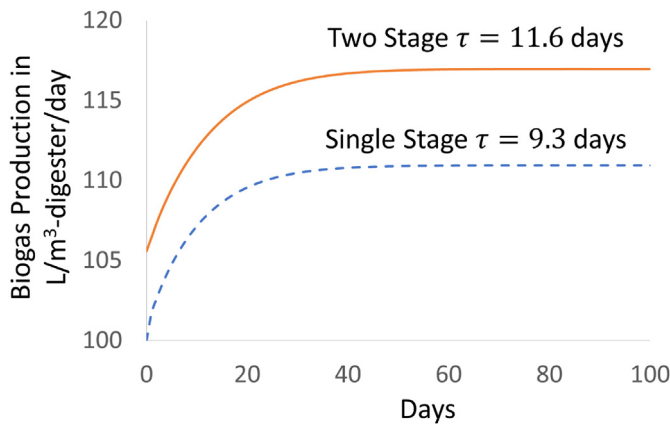


Fig. 16. Dynamic response times of single stage and two stage CSTRs (first stage at 80% of total volume) of 1 m³ volume. The dynamic response as they attain their new steady state is shown. τ is the dynamic response time constant for first order response.

Once it is full, the digestate is withdrawn until the volume of the digestate reaches $V_{min} = 0.1 \text{ m}^3$. Fig. 18 shows the concentration of acidogens and acetomethanogens in the reactor's liquid phase as a function of time. Both microbial consortia stabilize at concentrations of 175 Units/m³ and 5.8 Units/m³ respectively. These are an order of magnitude greater than the concentrations in the continuous reactors.

Fig. 19 shows gas production for the semi-batch operation. The biogas production stabilizes at an average of 153 L of biogas per m³ of digester per day with an average methane percentage of 63%. Thus, the semi-batch operation which allows for a greater microbial concentration is clearly superior to continuous stirred reactor operation.

Fig. 20 shows the effect on the microbial concentration in the digester of varying the water lettuce to dung ratio as well as the overall feed rate. Increasing feed rate and increasing the fraction of water lettuce in the feed reduces the microbial concentration. Fig. 21 shows the corresponding methane production rate. The semi-batch approach is superior to the continuous stirred tank approach since it allows handling of greater microbial concentrations.

3.5. Economics of water lettuce grown on farm ponds

A number of farms incorporate a water reservoir – a farm-pond [26]. It is of interest to investigate the economic benefits of using the farm pond to grow aquatic macrophytes. Pond coverage by the macrophyte could minimize evaporation while simultaneously providing a source of feed for biogas production. The biogas could be monetized by using it for domestic cooking/heating in place of market bought LPG (liquefied petroleum gas) i.e. the savings can be considered gains. For this exercise, we will consider a farm pond of area $A_{pond} = 1000 \text{ m}^2$.

3.5.1. Water lettuce production

Water lettuce grows at 5.8 gm-dry mass/m²/day when cultivated [6]. The quantity of degradable biomass per kg of fresh water lettuce is $m_{pistia}^0 = 0.164 \text{ kg/kg}$ (from Table 4). The ash fraction in water lettuce is about 2% [1]. Hence, the drymass constitutes about 18.4% of water lettuce i.e. the production rate of fresh water-lettuce is $p_r = 0.0315 \text{ kg/m}^2/\text{day}$.

If R_{pistia} is the rate (in kg/day) at which fresh water-lettuce is fed to a digester, then for the farm pond taken for this exercise, $R_{pistia} = A_{pond} p_r = 31.5 \text{ kg/day}$.

3.5.2. Cost of digester

The digester is operated in the semi-batch manner described in Section 3.4. The digester is a cylindrical vessel made of oil-painted mild steel with height to diameter ratio of $h_{rat} = 1.3$ and with flat ends. The height of fluid to the diameter is $h_{rat}^{fluid} = 1$. The vessel is unpressurized; hence the thickness is $th_{vessel} = 0.004 \text{ m}$. The density of steel is taken to be $\rho_{steel} = 8000 \text{ kg/m}^3$. The cost for mild steel (including fabrication) is $c_{steel} = \$2/\text{kg}$. If d_{vessel} is the diameter of the vessel then the maximum volume (V_{fluid}^{max}) and minimum volume (V_{fluid}^{min}) of the fluid is:

$$V_{fluid}^{max} = \frac{\pi}{4} h_{rat}^{fluid} d_{vessel}^3 \quad V_{fluid}^{min} = 0.1 V_{fluid}^{max} \quad (23)$$

The cost of the vessel is:

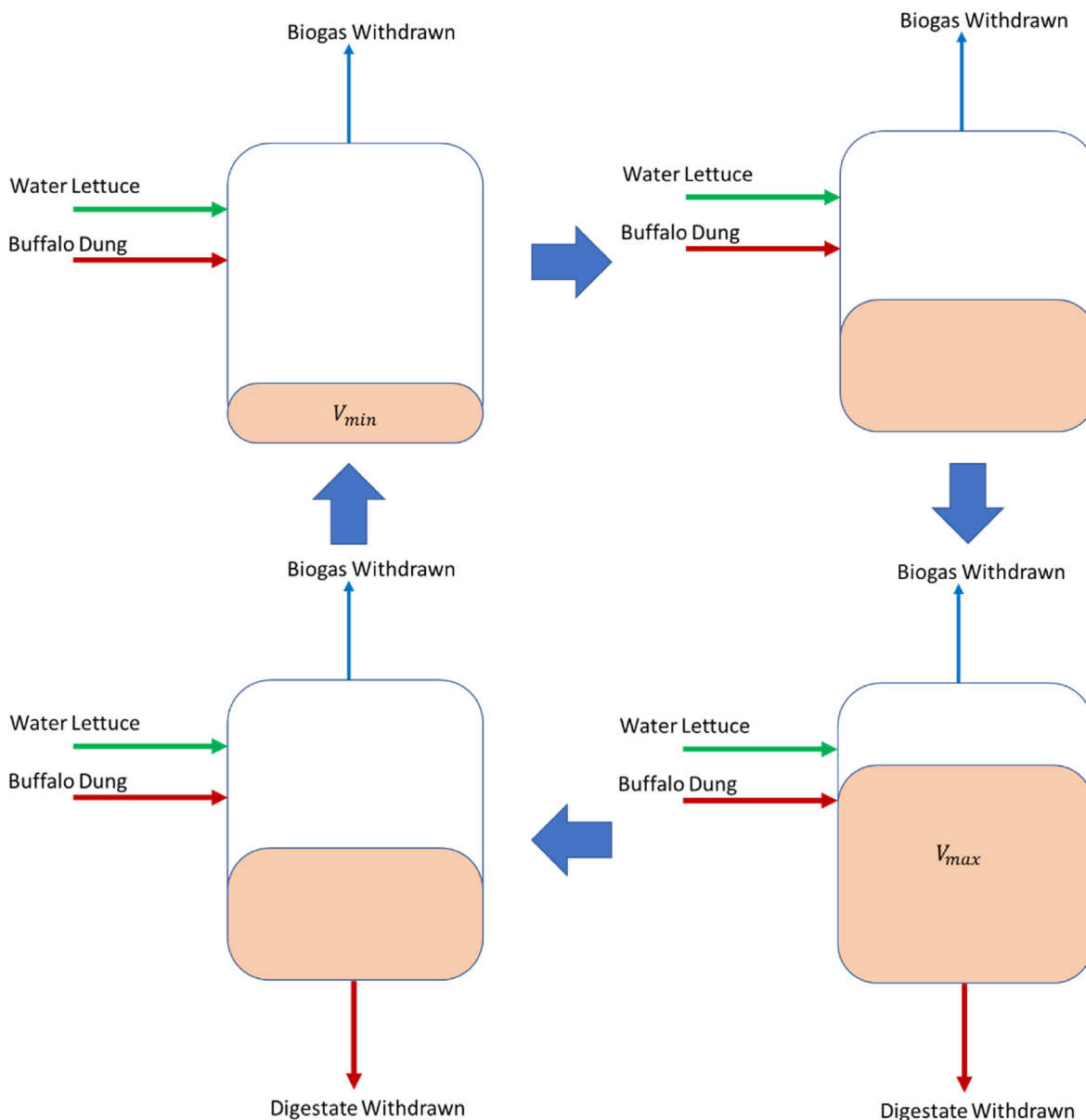


Fig. 17. Schematic of the semi batch operation described in Section 4.3. The feed was added and biogas was withdrawn continuously while the digestate was withdrawn intermittently.

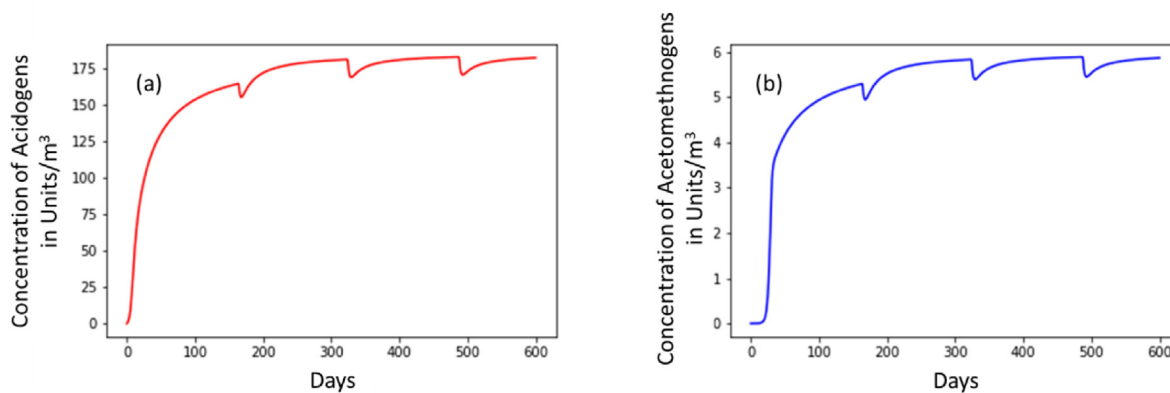


Fig. 18. Concentration of microbial consortia in units per m³ as a function of time in a semi batch digester of 1 m³ maximum volume with a feed consisting of 5 kg/day of fresh water lettuce, 0.5 kg/day of dung (a) Concentration of acidogens which stabilizes at 175 Units/m³ and (b) Concentration of acetomethanogens which stabilizes at 5.8 Units/m³.

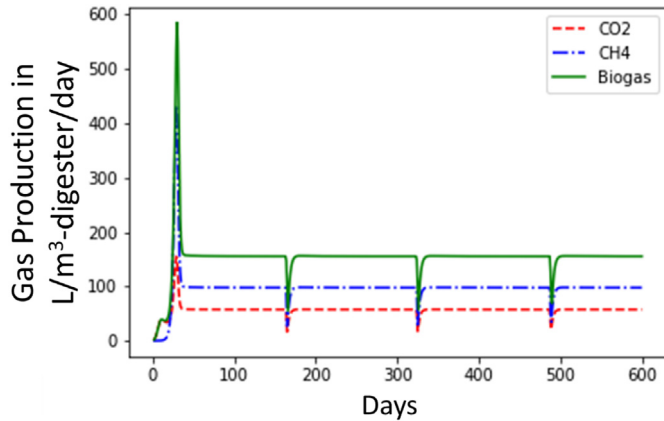


Fig. 19. Gas production as a function of time for the semi-batch operation.

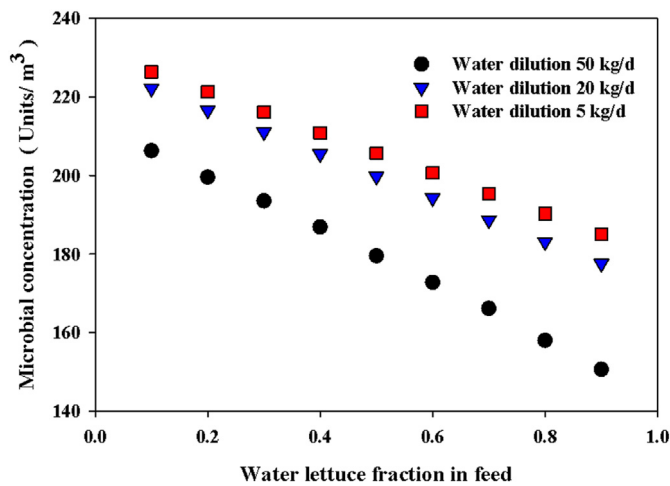


Fig. 20. Microbial Concentration in 1 m³ biodigester operated semi-batch wise for different fractions of water lettuce in a feed comprising water lettuce and dung. The parameter is the total feed rate of water-lettuce + dung.

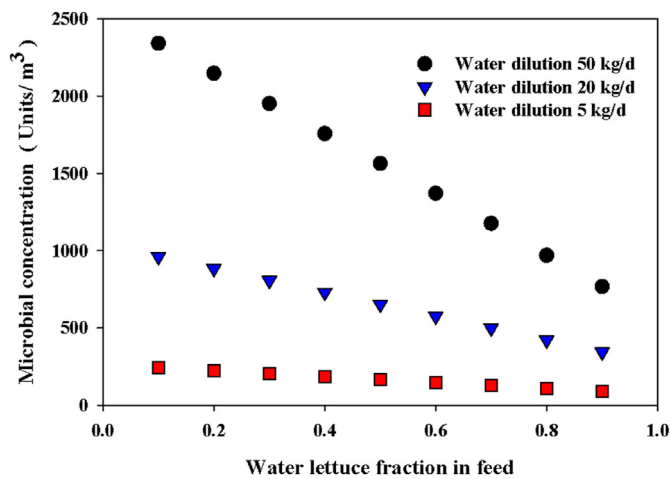


Fig. 21. Methane production in 1 m³ biodigester operated semi-batch wise for different fractions of water lettuce in a feed comprising water lettuce and dung. The parameter is the total feed rate of water-lettuce + dung.

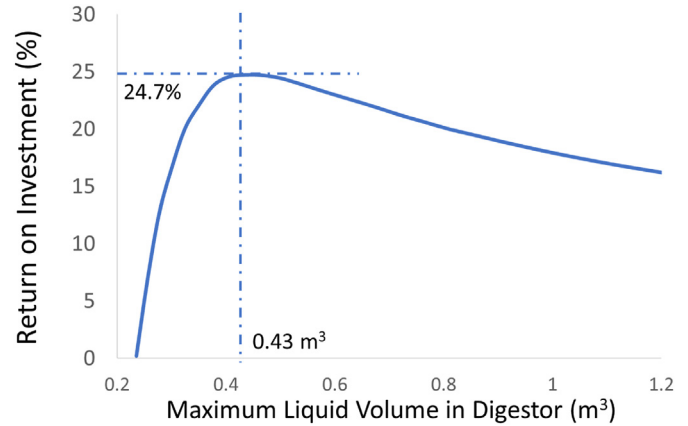


Fig. 22. Return on Investment vs Maximum Liquid Volume in Digester. The curve features an optimum at 0.43 m³ corresponding to a return on investment of 24.7%.

$$C_{vessel} = \left(\frac{1}{2} + h_{rat} \right) \pi d_{vessel}^2 t_{vessel} \rho_{steel} C_{steel} \quad (24)$$

3.5.3. Cost of LPG and LPG equivalent

According to a major supplier [27], the cost of a 14.2 kg LPG cylinder is about \$10. i.e. LPG costs $C_{LPG} = \$0.7/\text{kg}$. The lower heating value of LPG is 45.5 MJ/kg while that of methane is 50.0 MJ/kg. Hence 1 kg of methane is equivalent to 1.1 kg of LPG i.e. $\eta_{eq} = 1.1$.

3.5.4. Return on investment

Let F_{CH_4} be the daily rate of production of methane in kg/day. Assuming the digester is operated continuously for $Y = 330$ days a year the yearly savings from this operation are:

$$C_{CH_4} = F_{CH_4} Y \eta_{eq} C_{LPG} \quad (25)$$

Hence, the return on investment is:

$$RoI = \frac{C_{CH_4}}{C_{vessel}} \quad (26)$$

Note that labour and machinery specifically for this is not considered since operating the digester is not exceptionally demanding of man hours compared to other farm labour and a farm hand can be directed to operate it on existing pay using the idle time of existing farm machinery.

Fig. 22 shows the return on investment as a function of V_{max} . The optimum shows a 24.7% return on investment at $V_{max} = 0.43 \text{ m}^3$. For these conditions, $F_{CH_4} = 0.24 \text{ kg/day}$ with total biogas rate of 566 l/day with 58.5 vol% CH₄. The cost of the vessel is \$244 while the yearly revenue from savings on LPG is \$60.3. The optimum payback period is therefore just over 4 years.

3.6. Greenhouse gas emission mitigation

The substitution of fossil-fuel based LPG with renewable biogas from anaerobic digestion of water lettuce also has environmental benefits. Here is presented a simple life cycle analysis (LCA) which investigates the impact of substituting LPG as cooking fuel with biogas with a focus on greenhouse gas (GHG) emission implications. The study aligns itself with the scale applied in the economic

investigation of section 4.4.

The study considers the abated emissions from both the combustion and lifecycle of the pistia generated biogas against those of LPG's ($\dot{m}_{LPGcombustion,CO_2}$ and $\dot{m}_{LPGlifecycle,CO_2}$). The latter term includes LPG's extraction, refining, bottling and transport. During combustion, LPG releases 3.01 kg CO₂/kg of LPG, whilst bottled LPG in India is said to emit 0.122 kg CO₂/kg during its lifecycle [28].

The lifecycle emissions of the anaerobic digester's construction material, comprised of 122 kg of mild steel for a total biomethane generation of 79.2 kg/yr, have also been taken into account with both its embedded emissions from production ($\dot{m}_{MildSteelEmbedded,CO_2}$) and from its transport to site ($\dot{m}_{MildSteelTransport,CO_2}$). An emission factor of 2 kg CO₂ per kg of mild steel was used for the embedded emissions as stipulated in Argonne National Laboratory's (ANL) GREET LCA software ([29]).

The transport distance for the steel from production plant to AD site ($d_{travelled,steel}$) was calculated using the number of integrated steel works in India ($N_{integrated\ steel\ plants}$), assigning them theoretical coverage areas from India's total land area (A_{India}) and estimating the travel distance ($d_{travelled,steel}$) as the radius of these areas of coverage equation [27]). India has 13 large-scale integrated steel plants which produce the vast majority of mild steel in the country [30].

$$d_{travelled,steel} = \sqrt{\frac{A_{India}}{N_{integrated\ steel\ plants}}} \times \frac{1}{\pi} \quad (27)$$

The distance travelled by a heavy duty vehicle (HDV) lorry was speculated at 90% of the total distance with an emission factor of 0.125 g CO₂/(kg.km) [31].

$$\dot{m}_{totalCO_2} = t_{lifetime} (\dot{m}_{LPGcombustion,CO_2} + \dot{m}_{LPGlifecycle,CO_2}) - (\dot{m}_{MildSteelEmbedded,CO_2} + \dot{m}_{MildSteelTransport,CO_2}) \quad (28)$$

The total emission savings ($\dot{m}_{totalCO_2}$) were provided via calculation of equation [28] with a plant lifetime ($t_{lifetime}$) of 15 years.

The expected total GHG savings over the plant's lifetime are calculated to be 3.84 tonnes CO₂e. The majority of these savings arise from the abated emissions from LPG combustion ($\dot{m}_{LPGcombustion,CO_2}$) with 262 kg CO₂ saved annually compared to the 10.6 kg CO₂ annually abated from $\dot{m}_{LPGlifecycle,CO_2}$. The emissions from the digester's mild steel itself contributed just 244 kg CO₂, with 97% of this arising from the steel's embedded carbon emissions. The influence of the transport of steel from production plant to the AD site was minimal at just 6.6 kg CO₂. In conclusion, for this case study, the emissions savings per unit of water lettuce feedstock can be estimated at 0.025 kg CO₂e/kg water lettuce.

3.7. General observations

It must be noted that the above calculations are done on the basis of results obtained from ~1 L scale flasks and extrapolated to ~100–1000 L digesters. Such an extrapolation is done routinely in the process industry where kinetics obtained from laboratory scale experiments are extrapolated to pilot and commercial scales to determine techno-economic feasibility of a project. The main difference between chemical kinetics and biochemical kinetics involving a consortium of living organisms is the fact that the latter adapt to the changed circumstances of the larger vessels and perform differently. How they adapt is something that, of course, cannot be determined *a priori* however it is possible to make certain observations. The first is that the dimensions of the 1 L laboratory scale reactor are several orders of magnitude greater

than the dimensions of the microflora. Second, unlike in aerobic fermentations, mass transfer is not significantly different in a 1 L vessel from that in a 100 L vessel as long as the inputs are well mixed. Consequently, we can confidently assume that the 100–1000 L digester will behave approximately the same as the 1 L digester.

4. Conclusion

Water-lettuce (pistia stratiotes) was digested using buffalo dung as the inoculum. Five different water lettuce to inoculum ratios were tested. The gas analysis was done using a gas chromatograph and pressure was used instead of volume displacement to calculate the quantity of gas produced. A mechanistic model was proposed and fitted to the carbon dioxide and methane production data. Methane production required long lead times due to slow acclimatization of the microflora. However, once started, methane production ended in a span of only 20 days. Hence water lettuce inoculated with buffalo dung is an excellent source of high-quality biogas. The model has been used to simulate a 1 stage continuous digester and a 2 stage continuous digester. The 1 stage continuous digester can generate 100 L of biogas/m³-digester/day with methane fraction at 57%. It was discovered that, counter intuitively, the 2 stage digester was *not* a major improvement over the one stage digester. The latter gave only a 4% increase in methane production rate over the former while having a response time that was 25% longer. The approach that works best was the one that allows operation with high microbial concentrations. Since such sludges are not easily pumpable, a semi-batch approach is considered. Here feed is fed continuously and biogas withdrawn continuously but digestate is withdrawn intermittently. This seems to be the most promising option for getting high biogas production rates. If biogas, from water lettuce grown on a farm pond and generated by using the semi-batch approach, is used instead of buying LPG from the market, the savings are equivalent to a 24.7% return on investment and a payback period of just over four years. This corresponds to 25 kg of CO₂ abated per ton of fresh water lettuce utilized.

Credit author statement

G.N., S.R., V.H.D., A.R. conceived the manuscript. G.N. did the experiments. V.H.D. developed and calibrated the model and simulated the reactors with guidance from O.G., V.D. and A.P. O.G., V.D. did calculations for Greenhouse Gas Mitigation. All authors wrote the paper. V.H.D. edited the paper.

Declaration of competing interest

The authors declare no conflict of interest.

Acknowledgements

We gratefully acknowledge support from the BBSRC, UK via the BEFWAM grantRef: BB/S011439/1 through the GCRF, UK. The DOI for the associated data to this paper is <https://doi.org/10.5518/1086>.

Appendix A. Supplementary data

Supplementary data to this article can be found online at <https://doi.org/10.1016/j.energy.2021.122911>.

References

- [1] Gupta R, Tripathi P, Kumar R, Sharma A, Mishra A. Pistia stratiotes (jalkumbhi). Phcog Rev 2010;4(8):153.

- [2] Sharma BM, Sridhar MKC. The productivity of *Pistia stratiotes* L. in a eutrophic lake. *Environ Pollut Ecol Biol* 1981;24(4):277–89.
- [3] Sengupta M, Xie Y, Lopez A, Habte A, Maclaurin G, Shelby J. The national solar radiation data base (NSRDB). *Renew Sustain Energy Rev* 2018;89:51–60.
- [4] Erol M, Haykiri-Acma H, Küçükbayrak S. Calorific value estimation of biomass from their proximate analyses data. *Renew Energy* 2010;35(1):170–3.
- [5] Melis A. Solar energy conversion efficiencies in photosynthesis: minimizing the chlorophyll antennae to maximize efficiency. *Plant Sci* 2009;177(4):272–80.
- [6] Olguín EJ, García-López DA, González-Portela RE, Sánchez-Galván G. Year-round phytofiltration lagoon assessment using *Pistia stratiotes* within a pilot-plant scale biorefinery. *Sci Total Environ* 2017;592:326–33.
- [7] Martínez-Gutiérrez E. Biogas production from different lignocellulosic biomass sources: advances and perspectives. *Apr* 30 [cited 2020 Mar 18] *3 Biotech* 2018;8(5). Available from: <http://link.springer.com/10.1007/s13205-018-1257-4>.
- [8] Abbasi SA, Nipanay PC, Panholzer MB. Biogas production from the aquatic weed *Pistia stratiotes*. *Bioresour Technol* 1991;37(3):211–4.
- [9] Kumar V, Singh J, Pathak VV, Ahmad S, Kothari R. Experimental and kinetics study for phytoremediation of sugar mill effluent using water lettuce (*Pistia stratiotes* L.) and its end use for biogas production [Internet] *3 Biotech* 2017;7(5) [cited 2020 Mar 14], <http://link.springer.com/10.1007/s13205-017-0963-7>.
- [10] Fernandes KD, Cañote SJB, Ribeiro EM, Thiago Filho GL, Fonseca AL. Can we use Cd-contaminated macrophytes for biogas production? *Environ Sci Pollut Control Ser* 2018;26(27):27620–30.
- [11] Nipanay PC, Panholzer MB. Influence of temperature on biogas production from *Pistia stratiotes*. *Biol Waste* 1987;19(4):267–74.
- [12] Güngören Madenoğlu T, Jalilnejad Falizi N, Kabay N, Güneş A, Kumar R, Pek T, et al. Kinetic analysis of methane production from anaerobic digestion of water lettuce (*Pistia stratiotes* L.) with waste sludge. *J Chem Technol Biotechnol* 2019;94(6):1893–903.
- [13] Batstone DJ, Keller J, Angelidaki I, Kalyuzhnyi SV, Pavlostathis SG, Rozzi A, et al. The IWA anaerobic digestion model No 1 (ADM1). *Water Sci Technol* 2002;45(10):65–73.
- [14] Donoso-Bravo A, Mailier J, Martin C, Rodríguez J, Aceves-Lara CA, Wouwer AV. Model selection, identification and validation in anaerobic digestion: a review. *Water Res* 2011;45(17):5347–64.
- [15] Lauwers J, Appels L, Thompson IP, Degrève J, Van Impe JF, Dewil R. Mathematical modelling of anaerobic digestion of biomass and waste: power and limitations. *Prog Energy Combust Sci* 2013;39(4):383–402.
- [16] Adl M, Sheng K, Gharibi A. Examining a pretty simple and low cost method for modeling of biogas production from biodegradable solids. *Energy Proc* 2015;75:748–53.
- [17] Filer J, Ding HH, Chang S. Biochemical methane potential (BMP) assay method for anaerobic digestion research. *Water* 2019;11(5):921.
- [18] Seswoya R, Fen AS, Yang LK, Sulaiman SM. Performance of anaerobic digestion of fruit and vegetable waste (FVW). *AIP Conf Proc* 2019;2157(1):020026.
- [19] Jingura RM, Kamusoko R. Methods for determination of biomethane potential of feedstocks: a review. *Biofuel Res J* 2017;4(2):573–86.
- [20] Vavilin VA, Fernandez B, Palatsi J, Flotats X. Hydrolysis kinetics in anaerobic degradation of particulate organic material: an overview. *Waste Manag* 2008;28(6):939–51.
- [21] Jones E, Oliphant T, Peterson P. Others. SciPy: open source scientific tools for Python. Available from: <http://www.scipy.org/>; 2001.
- [22] Branch MA, Coleman TF, Li Y. A subspace, interior, and conjugate gradient method for large-scale bound-constrained minimization problems. *SIAM J Sci Comput* 1999;21(1):1–23.
- [23] J S, Lohit Kumar SG, B R. Kinetic modeling of mixed culture process of anaerobic Co-digestion of vegetable wastes with *Pistia stratiotes*: a scientific attempt on biomethanationy [cited 2020 Mar 24] *J Microb Biochem Technol* 2017;9(1). Available from: <https://www.omicsonline.org/open-access/kinetic-modeling-of-mixed-culture-process-of-anaerobic-codigestionof-vegetable-wastes-with-pistia-stratiotes-a-scientific-attempt-1948-5948-1000341.php?aid=85908>.
- [24] Levenspiel O. *Chemical reaction engineering*. third ed. New York: Wiley; 1999.
- [25] Boe K, Angelidaki I. Serial CSTR digester configuration for improving biogas production from manure. *Water Res* 2009;43(1):166–72.
- [26] Choudhury N, Tiwale S. Transforming livelihoods through farm ponds - the Hindu. *The Hindu* [Internet]. 2019. Aug 1 [cited 2020 Mar 31]; Available from: <https://www.thehindu.com/opinion/op-ed/transforming-livelihoods-through-farm-ponds/article28775209.ece>.
- [27] Indane cooking gas. Available from: <https://www.iocl.com/Products/Indanegas.aspx>; 2020.
- [28] Kaushik LK, Muthukumar P. Life cycle Assessment (LCA) and Techno-economic Assessment (TEA) of medium scale (5–10 kW) LPG cooking stove with two-layer porous radiant burner. *Appl Therm Eng* 2018;133:316–26.
- [29] GREET model. Argonne National Laboratory; 2012.
- [30] Hyvonen M, Langcake S. India's steel industry. Reserve Bank of Australia; 2012. p. 29. –35. Available from: <https://ideas.repec.org/a/rba/rbabul/mar2012-04.html>.
- [31] Schaeffer R, Sims REH, Corfee-Morlot J, Creutzig F, Cruz-Nunez X, Dimitriu D, et al. Transport. Economic evaluation of climate change impacts [internet]. Cham: Springer International Publishing; 2015. cited 2020 Apr 22]. pp. 279–300. Available from: http://link.springer.com/10.1007/978-3-319-12457-5_15.